

Radiative Effects in the Processes of Hadron Electroproduction

I.Akushevich, N.Shumeiko, A.Soroko

National Center of Particle and High Energy Physics, 220040 Minsk, Belarus

Received: date / Revised version: date

Abstract. An approach to calculate radiative corrections to unpolarized cross section of semi-inclusive electroproduction is developed. An explicit formulae for the lowest order QED radiative correction are presented. Detailed numerical analysis is performed for the kinematics of experiments at the fixed targets.

1 Introduction

Semi-inclusive processes of hadron electroproduction have been recognized long ago [1] as an important tool for testing QCD predictions of nucleon structure because they admit to get information about quark distributions in the nucleon for each flavour separately. Precise analysis of the hadron structure functions extracted from the experimental data requires, however, an iterative procedure involving radiative correction (RC) of these data. RC to cross section of semi-inclusive processes can be calculated on basis of Bardin and Shumeiko covariant approach offered in ref.[2] originally for elastic scattering. In ref.[3] the method was developed on semi-inclusive processes, where analytical formulae for the lowest order RC for coincident processes in electroproduction were found. In this paper we present analogous formulae, but in contrary to results of the ref.[3] we do not assume integration over hadronic kinematical variables p_t^2 and ϕ^h . It allows to calculate the model-independent RC relying only on the common representation for the hadronic tensor.

Last years the cross sections of the hadron electroproduction on fixed targets were measured as functions of azimuthal angles and transversal momentum of registered particles (see [4] and references therein). However this information is not sufficient to extract all structure functions involved in the hadronic tensor in wide kinematical region required for RC calculation. Therefore we have to use some model for the semi-inclusive structure functions. Such a model should give a good initial approximation for the iterative procedure, and we hope that the model for structure functions, which can be constructed on the basis of results of Mulders and Tangerman [5], is an appropriate one. It should be noted that unpolarized structure functions were considered in [5] along with the spin dependent distributions. However, in this paper we restrict ourselves only by calculation of RC to unpolarized cross section, and the consideration of RC to observable quantities in polarization experiments on hadron electroproduction will be a subject of a separate publication. Notice that for az-

imuthal effects we use additionally a model given in ref.[6] (see also [7]).

In the Section 2 we shortly describe the kinematics of the hadron electroproduction process with and without radiation of additional photon. The hadronic tensor and the model for structure functions are discussed in Section 3. The analytical formulae for Born cross section and for RC of the lowest order are given in Sections 3 and 4. In this paper the only ultrarelativistic approximation is made: electron mass is considered to be small. We note that final analytical formulae are written in the form similar to used in FORTRAN code POLRAD 2.0 [8]. The Section 5 is devoted to numerical analysis, performed on the basis of new code HAPRAD specially developed by us for this purpose. Most cumbersome formulae are gathered in the Appendix.

2 The kinematics

The cross section of hadron h electroproduction

$$e(k_1) + N(p) \longrightarrow e'(k_2) + h(p_h) + X(p_x) \quad (1)$$

depends on five kinematical variables which can be chosen as

$$x, y; z, t, \phi_h, \quad (2)$$

where x and y are usual scaling variables, z and t are defined via hadron momentum

$$t = (q - p_h)^2, \quad z = p_h p / pq, \quad q = k_1 - k_2, \quad (3)$$

ϕ_h is an angle between planes $(\mathbf{k}_1, \mathbf{k}_2)$ and $(\mathbf{q}, \mathbf{p}_h)$ in the rest frame ($p = (M, \mathbf{0})$). Also the following invariants will be used

$$\begin{aligned} S &= 2k_1 p, \quad X = 2k_2 p = (1 - y)S, \quad Q^2 = -q^2 = xyS, \\ W^2 &= S_x - Q^2 + M^2, \quad S_x = S - X, \quad S_p = S + X, \\ \lambda_Q &= S_x^2 + 4M^2 Q^2, \\ M_x^2 &= p_x^2 = (1 - z)S_x + M^2 + t, \quad V_{1,2} = 2k_{1,2} p_h. \end{aligned} \quad (4)$$

When the radiative process

$$e(k_1) + N(p) \longrightarrow e'(k_2) + \gamma(k) + h(p_h) + X(\tilde{p}_x) \quad (5)$$

is considered, the three additional independent variables have to be introduced

$$R = 2kp, \quad \tau = qk/kp, \quad \phi_k, \quad (6)$$

ϕ_k is the rest frame angle between planes $(\mathbf{k}_1, \mathbf{k}_2)$ and (\mathbf{q}, \mathbf{k}) . Also we introduce the quantity $\mu = kp_h/kp$ and the following invariants

$$\begin{aligned} \tilde{Q}^2 &= (q - k)^2 = Q^2 + R\tau, \\ \tilde{W}^2 &= (p + q - k)^2 = W^2 - R(1 + \tau), \\ \tilde{t} &= (q - k - p_h)^2 = t + R(\tau - \mu), \\ \tilde{M}_x^2 &= \tilde{p}_x^2 = M_x^2 + R(1 + \tau - \mu). \end{aligned} \quad (7)$$

The phase space of the three final particles is parameterized as

$$\frac{d^3\mathbf{k}_2}{k_{20}} \frac{d^3\mathbf{p}_h}{p_{h0}} \frac{d^3\mathbf{k}}{k_0} = \pi S_x dx dy \frac{S_x dz dt d\phi_h}{2\sqrt{\lambda_Q}} \frac{RdRd\tau d\phi_k}{\sqrt{\lambda_Q}}. \quad (8)$$

Instead of t -dependence we will also consider the cross section as a function of transversal momentum p_t defined in (A.8).

We are interesting in explicit dependence on angles ϕ_h and ϕ_k . So it is useful to take the some scalar products with p_h in the form

$$\begin{aligned} \frac{1}{2}V_{1,2} &= k_{1,2}p_h = a^{1,2} + b \cos \phi_h, \\ \frac{1}{2}\mu R &= kp_h = R(a^k + b^k(\cos \phi_h \cos \phi_k + \sin \phi_h \sin \phi_k)). \end{aligned} \quad (9)$$

Also we will use $a^\pm = a^2 \pm a^1$. The explicit expressions for coefficients are given in Appendix (A.7).

3 The hadronic tensor and the Born approximation

The cross section of the electroproduction process can be obtained in terms of convolution of leptonic and hadronic tensors. There are two leptonic tensors: with and without additional radiated photon. The Born leptonic tensor (without a photon) is standard, and radiative one is cumbersome. The explicit expressions for the leptonic tensors and formulae for RC in terms of them can be found in [9,10].

The hadronic tensor without the T - and P -odd terms can be presented in the form [11,12]

$$W^{\mu\nu} = -\tilde{g}^{\mu\nu}\mathcal{H}_1 + \tilde{p}^\mu\tilde{p}^\nu\mathcal{H}_2 + \tilde{p}_h^\mu\tilde{p}_h^\nu\mathcal{H}_3 + (\tilde{p}^\mu\tilde{p}_h^\nu + \tilde{p}_h^\mu\tilde{p}^\nu)\mathcal{H}_4, \quad (10)$$

where

$$\tilde{g}^{\mu\nu} = g^{\mu\nu} + \frac{q^\mu q^\nu}{Q^2}, \quad \tilde{p}^\mu = p^\mu + \frac{q^\mu pq}{Q^2}, \quad \tilde{p}_h^\mu = p_h^\mu + \frac{q^\mu p_h q}{Q^2}, \quad (11)$$

and all of the SF depend on four kinematical invariants (for example, Q^2, W^2, t, z) The model for structure functions can be constructed on basis of results of the paper Mulders and Tangerman [5]. Keeping only the leading twist contribution we have for structure functions

$$\begin{aligned} \mathcal{H}_1 &= \sum_q e_q^2 f_q(x) D_q \mathcal{G}, \\ \mathcal{H}_2 &= -\frac{p_t^2 + m_h^2}{M^2 E_h^2} \sum_q e_q^2 f_q(x) D_q \mathcal{G}, \\ \mathcal{H}_3 &= 0, \\ \mathcal{H}_4 &= \frac{1}{ME_h} \sum_q e_q^2 f_q(x) D_q \mathcal{G}, \end{aligned} \quad (12)$$

and

$$\mathcal{G} = \mathcal{G}_1 = b \exp(-bp_t^2), \quad (13)$$

where $b = R^2/z^2$ is a slope parameter and R is a parameter of the model.

The Born cross section has the following dependence on ϕ_h :

$$\sigma_0 = \frac{d\sigma_0}{dx dy dz dp_t^2 d\phi_h} = \frac{N}{Q^4} (A + \cos \phi_h A^c + \cos 2\phi_h A^{cc}), \quad (14)$$

where $N = \alpha^2 y S_x / \sqrt{\lambda_Q}$. The coefficients A do not depend on ϕ_h more and they have the form

$$\begin{aligned} A &= 2Q^2 \mathcal{H}_1 + (SX - M^2 Q^2) \mathcal{H}_2 \\ &\quad + (4a^1 a^2 + 2b^2 - M_h^2 Q^2) \mathcal{H}_3 \\ &\quad + (2Xa^1 + 2Sa^2 - zS_x Q^2) \mathcal{H}_4, \\ A^c &= 2b(2a^+ \mathcal{H}_3 + S_p \mathcal{H}_4), \\ A^{cc} &= 2b^2 \mathcal{H}_3. \end{aligned} \quad (15)$$

When integrated over the kinematical variables ϕ_h and p_t the cross section (14) coincides with the well known formula for semi-inclusive cross section calculated within QPM

$$\sigma_{xyz} = \frac{d\sigma}{dx dy dz} = \frac{2\pi\alpha^2}{yQ^2} (y^2 + 2 - 2y) \sum_q e_q^2 f_q(x) D_q. \quad (16)$$

Unfortunately, the p_t^2 distribution

$$\frac{1}{\sigma_{xyz}} \frac{d\sigma_{xyz}}{p_t^2} \approx \mathcal{G}, \quad (17)$$

calculated with the exponential slope (13) does not fit experimental data with sufficient χ^2 . So the more complicated model [13] with power dependence on p_t^2 seems to be more adequate. Another possibility to come to an agreement with the data consists in replacement of the Gaussian factor (13) by the fit of experimental p_t^2 -distribution taken in the form [4]

$$\mathcal{G} = \mathcal{G}_2 = \left[\frac{1}{a + bz + p_t^2} \right]^{c+dz}. \quad (18)$$

x	y	Q^2 GeV ²	z	SIRAD	HAPRAD					
					without cuts			with cuts		
					\mathcal{G}_1	\mathcal{G}'_1	\mathcal{G}_2	\mathcal{G}_1	\mathcal{G}'_1	\mathcal{G}_2
0.038	0.677	1.33	0.25	1.029	1.033	1.024	0.982	1.041	1.025	0.985
0.062	0.567	1.82	0.35	0.996	0.989	0.989	0.947	0.989	0.980	0.951
0.092	0.529	2.52	0.45	0.970	0.961	0.961	0.934	0.961	0.956	0.936
0.131	0.499	3.38	0.55	0.945	0.936	0.933	0.912	0.934	0.931	0.906
0.198	0.476	4.88	0.65	0.918	0.902	0.902	0.889	0.897	0.897	0.881

Table 1. The results for RC factors to three dimensional semi-inclusive cross section obtained using FORTRAN codes SIRAD and HAPRAD (see text for further explanations). Kinematical points are taken from the Table 1 of ref.[17].

4 The radiative correction of the lowest order

The cross section that takes into account radiative effects can be written as

$$\sigma_{obs} = \sigma_0 e^{\delta_{inf}} (1 + \delta_{VR} + \delta_{vac}) + \sigma_F. \quad (19)$$

Here the corrections δ_{inf} and δ_{vac} come from radiation of soft photons [14] and effects of vacuum polarization¹. The correction δ_{VR} is infrared free sum of factorized parts of real and virtual photon radiation. These quantities are given by the following expressions

$$\begin{aligned} \delta_{VR} &= \frac{\alpha}{\pi} \left(\frac{3}{2} l_m - 2 - \frac{1}{2} \ln^2 \frac{X'}{S'} + \text{Li}_2 \frac{S'X' - Q^2 p_x^2}{S'X'} - \frac{\pi^2}{6} \right), \\ \delta_{inf} &= \frac{\alpha}{\pi} (l_m - 1) \ln \frac{(p_x^2 - (M + m_\pi)^2)^2}{S'X'}, \\ \delta_{vac} &= \delta_{vac}^{lept} + \delta_{vac}^{hadr}, \end{aligned} \quad (20)$$

where $S' = X + Q^2 - V_2$, $X' = S - Q^2 - V_1$, $l_m = \ln Q^2/m^2$ and Li_2 is Spence function or dilogarithm.

The contribution of radiative tail has the standard form [15,10]

$$\begin{aligned} \sigma_F &= -\frac{\alpha N}{2\pi} \int_0^{2\pi} d\phi_k \int_{\tau_{min}}^{\tau_{max}} d\tau \sum_{i=1}^4 \sum_{j=1}^3 \theta_{ij}(\tau, \phi_k) \times \\ &\times \int_0^{R_{max}} dR R^{j-2} \left[\frac{\mathcal{H}_i}{(Q^2 + R\tau)^2} - \delta_j \frac{\mathcal{H}_i^0}{Q^4} \right]. \end{aligned} \quad (21)$$

Here $2M^2\tau_{max,min} = S_x \pm \sqrt{\lambda_Q}$ and $R_{max} = (M_x^2 - (M + m_\pi)^2)/(1 + \tau - \mu)$, $\delta_j=1$ for $j=1$ and $\delta_j=0$ otherwise. The explicit formulae for functions $\theta(\tau, \phi_k)$ can be found in Appendix. The structure functions \mathcal{H}_i^0 have to be calculated for Born kinematics, but \mathcal{H}_i is calculated in terms of tilde variables (7).

5 Numerical analysis

In this section we give numerical results for RC to semi-inclusive unpolarized cross section. For all cases RC factor

¹ There are explicit formulae for leptonic contribution to vacuum polarization effect (see [15] for example) and parameterization of hadronic one [16].

is defined as a ratio of observed to born cross sections. Also we will speak about relative RC (or simply RC), which is difference between observed and born cross sections or asymmetries divided on Born ones.

For definiteness we choose the kinematics of experiment HERMES at DESY. First, HERMES is the modern current experiment with rich possibilities for studies in semi-inclusive physics (see [17]). Second, HERMES is the experiment with electron beam, so the relatively large RC in respect to muon DIS experiment are anticipated.

The dependence of RC on x , y and z is widely discussed in ref.[3], where quark-parton model was assumed. Similar results can be obtained using the formulae of this paper after integration over p_t and θ_h . In this paper we concentrate on comparison of the codes constructed on basis of the two sets of formulae and on studying of the effects beyond the quark-parton model: azimuthal asymmetries and dependencies on transversal momentum p_t .

5.1 FORTRAN codes POLRAD 2.0 and HAPRAD

The special FORTRAN code HAPRAD was developed to calculate the RC to five-dimensional cross section $d^5\sigma/dxdydzdp_t^2d\theta_h$. From the other hand there is the code POLRAD 2.0 with special patch SIRAD, which calculated RC to semi-inclusive three dimensional cross section obtained in QPM.

In this section we show that numerical results for RC to $d\sigma/dxdydz$ reproduced by these two codes coincide with a good accuracy. It can be seen from the Table 1. In the table we represent RC to the cross section as it follows from the runs of the codes POLRAD 2.0 and HAPRAD. Since HAPRAD allows one to take into account the kinematical cuts and to use different models for p_t^2 -slope, three fits for p_t^2 -distribution and the cases with and without experimental cuts were considered. The first fit for p_t^2 -slope is defined in (13), while the second and third ones are our fits of experimental data [4] using exponential ($\mathcal{G}'_1 = \mathcal{G}_1$ at $b = a/z$) and power (18) functional forms. As the kinematical cuts on ϕ_h and p_t of the measured hadron we took HERMES geometrical ones [18]. We can conclude from this analysis that neither important differences between SIRAD and HAPRAD results, if exponential model for p_t^2 -distribution is used, nor dependence on slope parameter model and applying of geometrical cuts are found. However RC takes a negative shift in the case of the model based on power

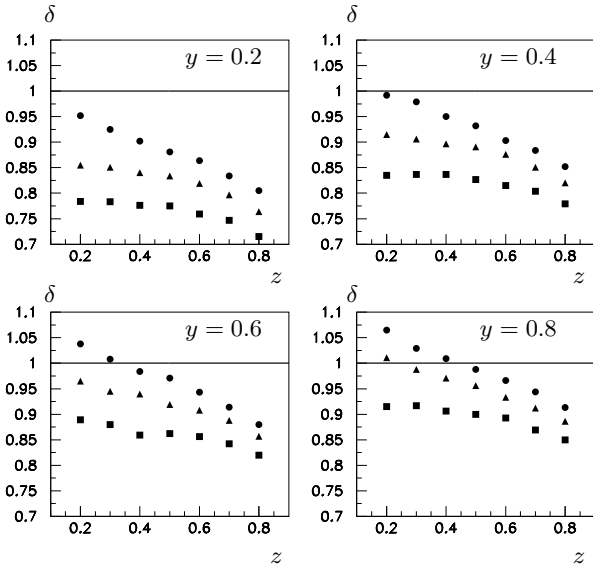


Fig. 1. Radiative correction to the semi-inclusive cross section for kinematics of HERMES; $\sqrt{S}=7.19$ GeV. Symbols from top to bottom correspond to the $x=0.05, 0.45$ and 0.7 . The results for $x=0.15$ are skipped, because they practically coincide with ones for $x=0.05$.

functional form (18). As it is discussed below RC depends on steepness of p_t^2 distribution. It is a reason why models like $\delta(p_t^2)$ (QPM, POLRAD 2.0) and (13) give larger RC. Within practical RC procedure in concrete measurement of $d\sigma/dxdydz$ the model can be fixed only if the information about p_t^2 -distribution is considered additionally.

Also two models for fragmentation function were considered: simple parameterization of the pion data [20] and modern model in the next-to-leading order QCD [21]. RC factor calculated using these models differs on several per cent. However this model dependence is less important because it can be eliminated by applying an iteration procedure, where fit of extracted data is used for RC calculation in subsequent step.

5.2 Cross section and $\langle p_t^2 \rangle$

Here we give numerical results for unpolarized cross section in kinematics of experiment HERMES [18]. RC factor (δ) to the semi-inclusive cross section integrated over p_t and ϕ_h as a function of x, y and z is presented in Figure 1. Further we analyse the z and p_t dependence of the cross section and azimuthal asymmetries. The dependencies of RC factor ($\bar{\delta} = \bar{\sigma}_{obs}/\bar{\sigma}_{born}$) to the semi-inclusive cross section on hadronic variables z and p_t are shown in Figure 2, where sigma bar ($\bar{\sigma}$) is meant the four-dimensional cross section $d\sigma/dxdydzdp_t^2$. We note that the obtained large correction to the cross section vs p_t is an analog of the similar results for vector meson electroproduction [10]. In our case the slope parameter depends on z (see (13)), so we have important z -dependence of the effect. However, if

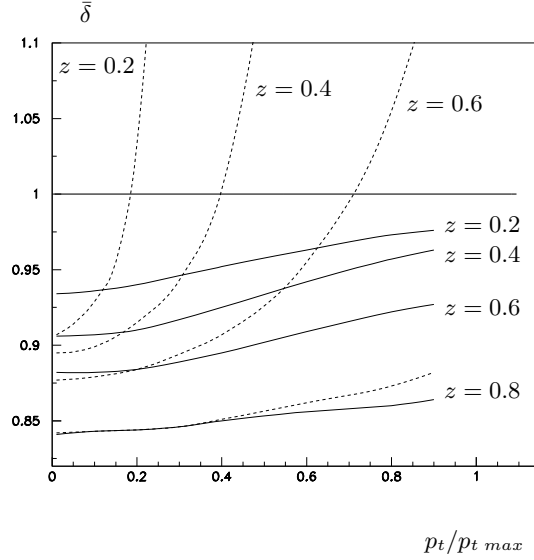


Fig. 2. Radiative correction to semi-inclusive cross section vs p_t ; $\sqrt{S}=7.19$ GeV, $x=0.15, Q^2=4$ GeV². Dashed and solid curves correspond to models (13) and (18) respectively.

the experimental fit for \mathcal{G} is used (solid curves in the Figure 2) there are no such a rise of RC for high p_t^2 values.

The crucial for QCD predictions [1] quantity $\langle p_t^2 \rangle$ is expressed in terms of $\bar{\sigma}$ as

$$\langle p_t^2 \rangle = \frac{\int dp_t^2 p_t^2 \bar{\sigma}}{\int dp_t^2 \bar{\sigma}}. \quad (22)$$

RC to this quantity can be expressed as

$$\begin{aligned} \delta_{pt} &= \frac{\int dp_t^2 p_t^2 \bar{\sigma}_{obs}}{\int dp_t^2 \bar{\sigma}_{obs}} \bigg/ \frac{\int dp_t^2 p_t^2 \bar{\sigma}_{born}}{\int dp_t^2 \bar{\sigma}_{born}} = \\ &= \frac{\int dp_t^2 p_t^2 \bar{\sigma}_{obs}}{\int dp_t^2 p_t^2 \bar{\sigma}_{born}} \frac{\int dp_t^2 \bar{\sigma}_{born}}{\int dp_t^2 \bar{\sigma}_{obs}} = \frac{\bar{\delta}_{pt}}{\delta}, \end{aligned} \quad (23)$$

where δ is semi-inclusive RC factor discussed above (see Figure 1). The correction $\bar{\delta}_{pt}$ both for exponential and power model (13,18) is presented on Figure 3.

Similar to the case of p_t^2 -distribution the radiative effect is larger when exponential model (13) is used. That is because of contribution of small \tilde{p}_t^2 when we integrate over the phase space of emitted photon (21). The steeper the slope of the p_t^2 -distribution the larger this contribution to RC.

5.3 Azimuthal asymmetries

The following azimuthal asymmetries are measurable in the experiments [19]

$$\langle \cos \phi_h \rangle = \bar{\sigma}_{obs}^{-1} \int_0^{2\pi} d\phi_h \cos \phi_h \sigma_{obs},$$

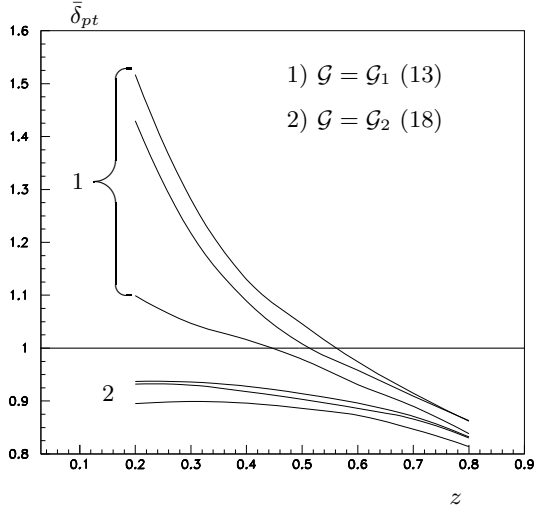


Fig. 3. Radiative correction to $\langle p_t^2 \rangle$ defined in eq. (23) for HERMES kinematics, $\sqrt{S}=7.19$ GeV, $y=0.4$. Curves from top to bottom corresponds to $x=0.15, 0.05$ and 0.45 .

$$\begin{aligned} \langle \cos 2\phi_h \rangle &= \bar{\sigma}_{obs}^{-1} \int_0^{2\pi} d\phi_h \cos 2\phi_h \sigma_{obs}, \\ \langle \sin \phi_h \rangle &= \bar{\sigma}_{obs}^{-1} \int_0^{2\pi} d\phi_h \sin \phi_h \sigma_{obs}. \end{aligned} \quad (24)$$

In terms of these quantities the observed cross section (19) can be written as

$$\begin{aligned} \sigma_{obs} &= \bar{\sigma}_{obs} (1 + \langle \cos \phi_h \rangle \cos \phi_h + \\ &\quad + \langle \cos 2\phi_h \rangle \cos 2\phi_h) + \sigma_{add}. \end{aligned} \quad (25)$$

Here σ_{add} is originated from contribution of higher harmonics ($\sin \phi_h, \sin 2\phi_h, \dots$). There are no their contributions at the Born level (see eq.14), and $\sigma_{add}^{Born} = 0$.

Azimuthal asymmetry $\langle \cos \phi_h \rangle$ is negative in considered region. RC to the quantity can exceed 10%. The result is done in Fig.4.

Within the model (12) $\langle \cos 2\phi_h \rangle$ is equal to zero at the Born level. So the asymmetry in this case is defined by RC only. Our estimation shows that this effect is of order 1%. Relative RC to the asymmetry can be estimated using another model [6], where $\langle \cos 2\phi_h \rangle \neq 0$ at the Born level. It is of order 10% in the region of applicability of the model.

$\langle \sin \phi_h \rangle$ is equal to zero at the Born level in any case. But there is nonzero contribution to it coming from RC. The numerical analysis shows that radiative corrections does not give visible contribution to it. For HERMES kinematical region values of $\langle \sin \phi_h \rangle$ does not exceed 0.01%.

We should stress that our predictions for the values of the radiative effects display a strong model dependence.

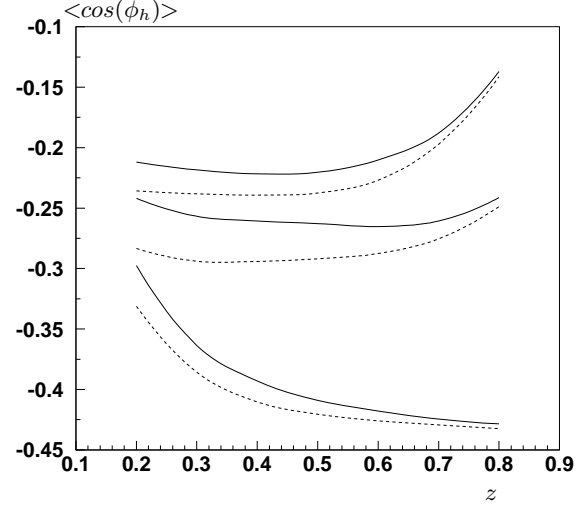


Fig. 4. Azimuthal asymmetry $\langle \cos \phi_h \rangle$ vs z for $y=0.2$ within HERMES kinematics; $\sqrt{S}=7.19$ GeV. Dashed (solid) lines correspond to born(observed) asymmetries. Curves from top to bottom correspond to $x=0.7, 0.45$ and 0.05 .

Therefore any reliable method of radiative correction of experimental data has to be based on an iterative procedure, where all necessary fits for RC codes use the processing data as an input and are specified in every step of this procedure. This procedure can be readily developed on the basis of the code HAPRAD.

6 Discussion and Conclusion

In this paper the QED radiative correction to different observable quantities in the experiments on hadron electroproduction is analyzed. The explicit covariant formulae are given in Section 4 and Appendix.

New FORTRAN code HAPRAD is developed in order to perform the numerical analysis. It was shown in Section 5.1 that the results for the RC to cross section integrated over p_t and ϕ_h are in agreement with POLRAD 2.0 [8]. Several models for structure functions and slope parameter in respect to p_t^2 were applied for. It is found that the model based on power p_t^2 -slope model leads to smaller values for RC.

Within the exponential model for \mathcal{G} (13) RC to $\langle p_t^2 \rangle$ can exceed 40%. However it essentially depends on the model of p_t^2 -distribution as well as on x and z .

RC to azimuthal asymmetries is of order 10%. The asymmetry $\langle \sin \phi_h \rangle$ due to RC is found to be negligible but not equaling to zero exactly.

FORTRAN code HAPRAD is available (aku@hep.by) for the calculation of RC to observable quantities in the experiments on the hadron electroproduction.

Acknowledgements

We are grateful to H.Avakian, A.Brull, H.Ihssen, R.Milner, K.Oganessyan and H.Spiesberger for fruitful discussions and comments.

Appendix

In this appendix we list the explicit form for functions θ_{ij} :

$$\theta_{ij}(\tau, \phi_k) = \theta_{ij}^0 + \cos \phi_k \theta_{ij}^c + \sin \phi_k \theta_{ij}^s + \cos 2\phi_k \theta_{ij}^{cc}, \quad (\text{A.1})$$

where

$$\theta_{12}^0 = 4\tau F_{IR},$$

$$\begin{aligned} \theta_{22}^0 = & -\frac{1}{2}F_d S_p^2 \tau + \frac{1}{2}F_{1+} S_p S_x \\ & + F_{2-} S_p + 2F_{2+} M^2 \tau \\ & - 2F_{IR} M^2 \tau + F_{IR} S_x, \end{aligned}$$

$$\begin{aligned} \theta_{32}^0 = & 2(-2F_d b^2 \tau - F_d (a^+)^2 \tau - F_{1+} a^- a^+ \\ & + 2F_{2-} \cos \phi_k b b^k + 2F_{2-} a^k a^+ \\ & - F_{IR} M_h^2 \tau - 2F_{IR} a^k a^-), \end{aligned}$$

$$\begin{aligned} \theta_{32}^c = & 4(-2F_d b a^+ \tau - F_{1+} b a^- + F_{2-} \cos \phi_k b^k a^+ \\ & + 2F_{2-} b a^k - \cos \phi_k F_{IR} b^k a^-), \end{aligned}$$

$$\theta_{32}^{cc} = 4b(-F_d b \tau + F_{2-} \cos \phi_k b^k),$$

$$\theta_{32}^s = 4b^k \sin \phi_k (F_{2-} a^+ - F_{IR} a^-),$$

$$\begin{aligned} \theta_{42}^0 = & -2F_d a^+ S_p \tau - F_{1+} a^- S_p + F_{1+} a^+ S_x \\ & + 2F_{2-} a^k S_p + 2F_{2-} a^+ + 2F_{2+} \tau z S_x \\ & + F_{IR} a^k S_x - 2F_{IR} a^- - 2F_{IR} \tau z S_x, \end{aligned}$$

$$\begin{aligned} \theta_{42}^c = & 2(-2F_d b S_p \tau + F_{1+} b S_x + F_{2-} \cos \phi_k b^k S_p \\ & + 2F_{2-} b + \cos \phi_k F_{IR} b^k S_x), \end{aligned}$$

$$\theta_{42}^s = 2b^k \sin \phi_k (F_{2-} S_p + F_{IR} S_x),$$

$$\theta_{13}^0 = -2(F + F_d \tau^2),$$

$$\theta_{23}^0 = 2FM^2 + F_d M^2 \tau^2 - \frac{1}{2}F_d S_x \tau - \frac{1}{2}F_{1+} S_p,$$

$$\begin{aligned} \theta_{33}^0 = & 2FM_h^2 + F_d M_h^2 \tau^2 + 2F_d a^k a^- \tau \\ & - 2F_{1+} \cos \phi_k b b^k - 2F_{1+} a^k a^+, \end{aligned}$$

$$\theta_{33}^c = 2(F_d \cos \phi_k b^k a^- \tau - F_{1+} \cos \phi_k b^k a^+ - 2F_{1+} b a^k),$$

$$\theta_{33}^{cc} = -2F_{1+} \cos \phi_k b b^k,$$

$$\theta_{33}^s = 2b^k \sin \phi_k (F_d a^- \tau - F_{1+} a^+),$$

$$\begin{aligned} \theta_{43}^0 = & 2FzS_x - F_d a^k S_x \tau + F_d a^- \tau + F_d \tau^2 z S_x \\ & - F_{1+} a^k S_p - F_{1+} a^+, \end{aligned}$$

$$\theta_{43}^c = -F_d \cos \phi_k b^k S_x \tau - F_{1+} \cos \phi_k b^k S_p - 2F_{1+} b,$$

$$\theta_{43}^s = -b^k \sin \phi_k (F_d S_x \tau + F_{1+} S_p). \quad (\text{A.2})$$

Here

$$F_{1+} = \frac{F}{z_1} + \frac{F}{z_2}, \quad F_{2+} = F \left(\frac{m^2}{z_2^2} + \frac{m^2}{z_1^2} \right),$$

$$F_{2-} = F \left(\frac{m^2}{z_2^2} - \frac{m^2}{z_1^2} \right), \quad F_d = \frac{F}{z_1 z_2}, \quad (\text{A.3})$$

where $F = 1/(2\pi\sqrt{\lambda_Q})$ and

$$F_{IR} = F_{2+} - Q^2 F_d. \quad (\text{A.4})$$

The quantities $z_{1,2} = k k_{1,2}/kp$ in terms of integration variables can be expressed as

$$\begin{aligned} z_1 = & \lambda_Q^{-1} (Q^2 S_p + \tau(SS_x + 2M^2 Q^2) - 2M \cos \phi_k \sqrt{\lambda_\tau \lambda}), \\ z_2 = & \lambda_Q^{-1} (Q^2 S_p + \tau(XS_x - 2M^2 Q^2) - 2M \cos \phi_k \sqrt{\lambda_\tau \lambda}), \end{aligned} \quad (\text{A.5})$$

where

$$\lambda_\tau = (\tau - \tau_{min})(\tau_{max} - \tau), \quad \lambda = SXQ^2 - M^2 Q^4 - m^2 \lambda_Q. \quad (\text{A.6})$$

The scalar products of p_h (9) are expressed via coefficients a^1, a^2, b, a^k and b^k :

$$\begin{aligned} 2Ma^1 = & SE_h - (SS_x + 2M^2 Q^2) p_l \lambda_Q^{-1/2}, \\ 2Ma^2 = & XE_h - (XS_x - 2M^2 Q^2) p_l \lambda_Q^{-1/2}, \\ b = & -p_t \sqrt{\lambda/\lambda_Q}, \\ 2Ma^k = & E_h - p_l (S_x - 2M^2 \tau) \lambda_Q^{-1/2}, \\ b^k = & -M p_t \sqrt{\lambda_\tau/\lambda_Q}. \end{aligned} \quad (\text{A.7})$$

The quantities E_h, P_l and P_t are invariants

$$\begin{aligned} E_h = & z\nu = \frac{zS_x}{2M}, \\ \frac{p_l \sqrt{\lambda_Q}}{M} = & t - M_h^2 + Q^2 + 2\nu E_h, \\ p_t^2 = & E_h^2 - p_l^2 - M_h^2. \end{aligned} \quad (\text{A.8})$$

In the rest frame they take sense of energy, longitudinal and transversal momenta of final hadron.

References

1. H.Georgi, H.D.Politzer, Phys. Rev. Lett. 40 (1978) 3.

2. D.Yu.Bardin, N.M.Shumeiko, Nucl. Phys. B127 (1977) 242.
3. A.V.Soroko, N.M.Shumeiko, Yad.Fiz. 49 (1989) 1348.
4. EMC Collab., J. Ashman et al, Z. Phys. C52 (1991) 361.
5. P.J. Mulders, R.D. Tangerman, Nucl. Phys. B461 (1996) 197, Erratum – ibid. B484 (1996) 538.
6. A. Brandenburg, V.V. Khoze, D. Muller, Phys. Lett. B347 (1995) 413.
7. K.A.Oganessyan, H.R.Avakian, N.Bianchi, P.Di Nezza Eu. Phys. J. C5 (1998) 681.
8. I.Akushevich, A.Ilyichev, N.Shumeiko, A.Soroko, A.Tolkachev, Comp. Phys. Comm. 104 (1997) 201.
9. I.V.Akushevich, A.N.Ilyichev and N.M.Shumeiko, J. Phys. G24 (1998) 1995.
10. I.Akushevich, hep-ph/9808309, *to be published in Eu. Phys. J. C*
11. K. Hagiwara, K. Hikasa, N. Kai Phys. Rev. D27 (1983) 84.
12. N.K.Pak, Ann. Phys. 104 (1977) 54.
13. R. Jakob, P.J. Mulders, J. Rodrigues, Nucl. Phys. A626 (1997) 937.
14. N.M.Shumeiko, Sov. J. Nucl. Phys. 29(1979)807.
15. I.V.Akushevich and N.M.Shumeiko, J. Phys. G20 (1994) 513.
16. H. Burkhardt, B. Pietrzyk, Phys. Lett. B356 (1995) 398.
17. HERMES Collab. K. Ackerstaff et al., Phys. Rev. Lett. 58 (1998) 5519.
18. HERMES. Technical design report, 1993.
19. EMC Collab., M. Arneodo et al, Z. Phys. C34 (1987) 277.
20. EMC Collab., J.J. Aubert *et al.* Phys. Lett. 160B (1985) 417.
21. J. Binnewies, B.A. Kniehl, G. Kramer, Z. Phys. C65 (1995) 471.